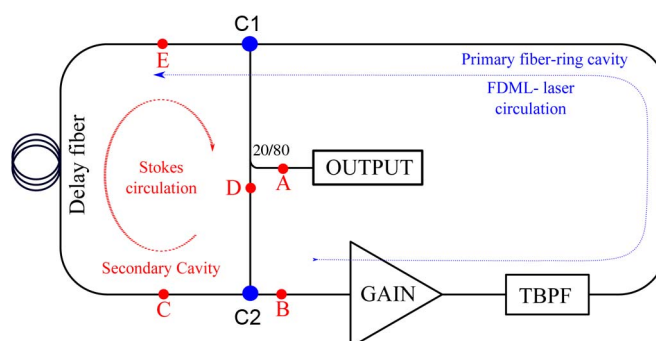


## Pulsed Wavelength-Tunable Brillouin Fiber Laser Based on a Fourier-Domain Mode-Locking Source

Volume 5, Number 4, August 2013

C. A. Galindez

J. M. Lopez-Higuera, Senior Member, IEEE



DOI: 10.1109/JPHOT.2013.2269795  
1943-0655/\$31.00 ©2013 IEEE

# Pulsed Wavelength-Tunable Brillouin Fiber Laser Based on a Fourier-Domain Mode-Locking Source

C. A. Galindez<sup>1,2</sup> and J. M. Lopez-Higuera,<sup>1</sup> *Senior Member, IEEE*

<sup>1</sup>Photonics Engineering Group, Universidad de Cantabria, 39005 Santander, Spain

<sup>2</sup>Physics Department, Universidade Federal de Pernambuco, 50670-901 Recife, Brazil

DOI: 10.1109/JPHOT.2013.2269795  
1943-0655/\$31.00 © 2013 IEEE

Manuscript received April 26, 2013; revised June 2, 2013; accepted June 6, 2013. Date of publication June 18, 2013; date of current version July 1, 2013. This work was supported by the Spanish government through project TEC2010-20224-C02-C02. Corresponding author: C. A. Galindez (e-mail: carlos.galindez@gmail.com).

**Abstract:** In this work, a pulsed wavelength-tunable Brillouin fiber laser based on a Fourier-domain mode-locking (FDML) source with a repetition rate of 4.2 kHz is presented. The tunable Brillouin laser is formed by a fiber-ring cavity (for the Stokes signal amplification) within a primary fiber-ring cavity for generating an FDML signal. The primary cavity is formed by an erbium-doped fiber amplifier and a fiber Fabry–Perot filter (FFP-F) as the gain medium and the tunable optical bandpass filter, respectively. A spectral laser tuning range of 2.54 nm centered in 1531 nm was achieved by adjusting the offset voltage of the FFP-F, while a variation, from 0.282 to 0.462 nm, on the Brillouin linewidth of the laser was achieved by setting the amplitude of a modulation signal applied in the FFP-F. A laser pulsewidth of 6.50  $\mu$ s was measured, and an output power of  $-7$  dBm was achieved.

**Index Terms:** Fiber lasers, Mode-locked laser, Tunable laser, Fiber non-linear optics.

## 1. Introduction

Brillouin fiber-ring cavity laser is a well-known laser configuration that has been intensively studied due to important features such as a narrow linewidth, low threshold power, gain quality of the nonlinear effect, and the easy experimental configuration [1]–[4]. These characteristics can be used for developing applications such as multiline lasers for temperature sensing [5] or gyroscopes [6]. The wavelength backward emitted corresponds to the Brillouin frequency shift ( $\nu_B$ ) from a given pump, in the order of ten gigahertz for 1550 nm, which is affected by physical and optical parameters of the optical fiber. A usual way for implementing this kind of lasers uses a distributed feedback (DBF) diode laser as the pumping source. In some applications, it is desirable to tune this wavelength, but the wavelength of DFB lasers can only be tuned about  $5 \times 10^{-2}$  nm/ $^{\circ}$ C and  $5 \times 10^{-4}$  nm/mA, limiting the wavelength range of the Brillouin laser operation.

On the other hand, the Fourier domain mode-locking (FDML) laser has recently become an attractive and powerful light source method, since the FDML laser allows high speed and broadband optical frequency sweeps [7]–[10]: features that are useful in areas such as optical coherent tomography (OCT) [7] and in optical fiber sensing [10], [11]. The implementation of FDML lasers is typically made by using a large gain medium and a narrowband optical filter. Some options for implementing the gain medium are the semiconductor optical amplifiers (SOAs) [7], the erbium-doped fiber amplifiers (EDFAs) [12], the Raman amplifiers [13], or the hybrid EDFA and optical parametric amplifiers [14]. Nonetheless, most of these configurations have been addressed to

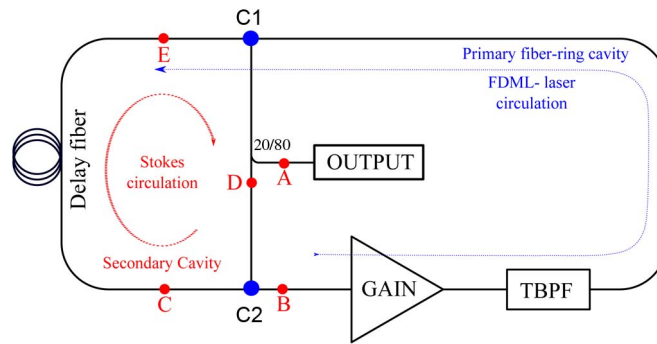


Fig. 1. Schematic of the double ring-cavity Brillouin-FDML laser.

enhance the gain media and to avoid effects such as stimulated Brillouin scattering into the ring-cavity [14].

Based on all the features above mentioned, it is really interesting to take advantage of both techniques and combine them, i.e., the Brillouin scattering and the mode-locking laser, for generating pulsed lasers with a high repetition rate, a broadband range and a set of Brillouin frequency shifts per pulse. Thus, a pulsed and wavelength-tunable Brillouin fiber laser pumped by an FDML source is proposed and experimentally demonstrated in this paper. The tunable laser here presented is basically formed by two fiber-ring cavities, a primary fiber-ring cavity, where the FDML signal is generated, and a secondary fiber-ring cavity, within the primary fiber-ring, which is used for amplifying the spontaneous Stokes signal caused by the FDML source.

## 2. Operation Principle of the Brillouin Laser FDML System Based

An FDML laser based on fiber-ring geometry consists of a fiber closed path with a gain medium, a tunable optical bandpass filter (TBPf), and a dispersion managed delay. The narrowband optical filter is tuned periodically at the cavity round-trip time  $\tau_{rt} = \tau_d + \delta_{tf} + \delta_{tg}$ , which mostly depends on the delay time  $\tau_d$  (related to the effective length of the fiber used as delay medium), the time  $\delta_{tf}$  that light takes to pass through the TBPf, and the time  $\delta_{tg}$  to pass through the gain medium. This tuning produces a quasi-stationary mode of operation. Thus, light from one frequency sweep propagates through the cavity and returns to the filter at the exact time when the transmission window of the optical band-pass filter is tuned to the same optical frequency. Therefore, light from the previous round-trip is coupled back to the gain medium, and the lasing does not have to build up from spontaneous emission.

The narrowband TBPf dissipates almost no energy because the back-coupled light contains only frequencies that are matched to the transmission window filter in each moment. In frequency domain, this requires destructive interference of all longitudinal modes that are not transmitted through the narrowband filter at a given time. Thus, the phases of the longitudinal modes must be locked. The laser output is not a train of short pulses; instead, it is a train of frequency sweeps or highly chirped, long pulses. The tunable narrowband filtering is equivalent to an infinite number of narrowband amplitude modulators that are slightly out of phase. Thus, spontaneous Brillouin scattering inside the ring-cavity can be generated, provided that the circulating power is above the threshold value, or that the delaying-fiber is long enough to reduce the threshold power. Besides, if the Brillouin scattering is self-reinforced with a ring-cavity, the Stokes generation will be more efficient and the emitted light will be related to the pump light from the FDML laser. In the case here exposed, a long delaying-fiber and a self-reinforced fiber-ring cavity were chosen for developing the laser.

A schematic diagram for describing the Brillouin-FDML laser is shown in Fig. 1. The path formed by the gain medium, the TBPf, and the delaying fiber constitutes the fiber-ring cavity for the FDML source. This cavity length ( $L_{FDML} = c\tau_{rt}/n$ ) depends on the cavity roundtrip and the light velocity

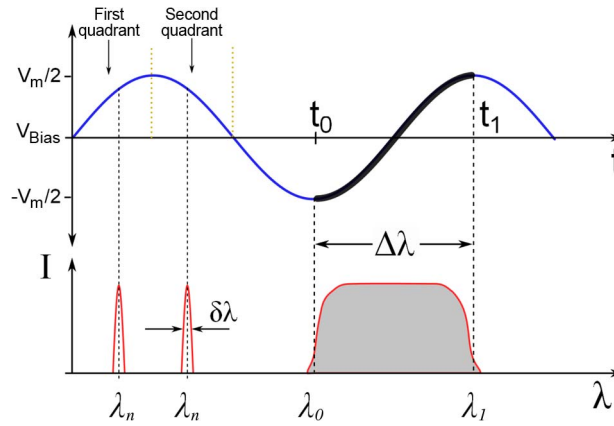


Fig. 2. Driven signal and wavelength generation in FDML lasers.

( $c/n$ ) and defines the optical roundtrip frequency that drives the TBPF. Light dispersion must be minimized so that different frequencies (or wavelengths) within the frequency sweep will propagate with the same roundtrip time; by using a “dispersion managed” delay, this condition is successfully accomplished. A fiber Fabry-Perot tunable filter (FFP-TF) can be used as the TBPF, which has simple structure and excellent optical properties. The wavelength  $\lambda_0$  in the FFP-TF is selected by setting a bias voltage tuning  $V_{Bias}$  ( $\lambda_0 \propto V_{Bias}$ ); then, the wavelength in the FDML ring-cavity can be easily tuned over a large range  $\Delta\lambda_{range}$ . The wavelength range is mostly limited by the gain medium.

Here, the FFP-TF is driven by a sinusoidal signal  $V_m \sin(2\pi f_d t)$  (driven frequency  $f_d$ ), with half frequency of the roundtrip frequency ( $f_{rt} = 2f_d$ ), because the values of wavelength selected by the FFP-TF at the first quadrant of  $\sin(2\pi f_d t)$  are the same selected at its second quadrant (see Fig. 2). This driven signal also defines the linewidth  $\Delta\lambda$  of the FDML laser by the expression

$$\Delta\lambda = C_\lambda V_m [\sin(2\pi f_d t_1) - \sin(2\pi f_d t_0)] \quad (1)$$

where,  $C_\lambda$  is a constant that relates the wavelength of the laser and the voltage in the FFP-TF;  $V_m$  is the amplitude of the sinusoidal signal;  $t_1$  and  $t_0$  are the time where the driven signal is maximized and minimized, respectively. If  $t_0$  is equal to  $(1/4f_d)$  and  $t_1$  to  $(3/4f_d)$ , then  $\Delta\lambda = -2C_\lambda V_m + C_\lambda V_{Bias}$  that is a multiple of the FFP-TF band-pass ( $\delta\lambda$ ). When  $V_m = 0$ ,  $\Delta\lambda$  is not zero, it is equal to  $\delta\lambda$  (see Fig. 2).

### 3. Experimental Details

To demonstrate the correct functioning of the Brillouin laser fed by an FDML system, the experimental setup is depicted in Fig. 3. This setup was implemented by using a fiber Fabry-Perot filter FFP-TF2 (Micron Optics Inc.), an EDFA BT17 (Photonics Inc.) working in the C-band,  $\sim 18.5$  km of single mode optical fiber, a polarization controller PC to compensate the polarization into the cavity, an Agilent generator 32250A, and a voltage source HP-E3631A. 80% of the circulating power of the Brillouin laser was taken out of the cavity. One half of this optical signal was directly monitored with an optical spectrum analyzer (OSA) Anritsu MS9030A, the other part was detected by a photodetector HP11982A for measuring the Brillouin frequency shift by using an electrical spectrum analyzer ESA HP-8562A.

The insertion of circulators in points C1 and C2 into the FDML fiber-cavity (see Fig. 1) allowed that the spontaneous Stokes scattering, which is generated in the optical fiber (used also as delaying fiber), could be re-injected as a contra-propagating seed for reinforcing the Brillouin scattering in the secondary cavity. This cavity was compounded by the path traced for the delaying fiber, ports 2, 3 of C1 and ports 1, 2 of C2. The non-transmitted pump power to the Stokes was guided by circulator 2 to the FFP-TF filter to complete the circulating process of light in the FDML

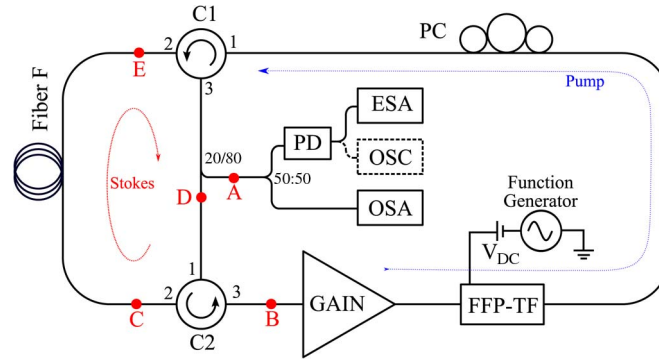


Fig. 3. Experimental setup developed for demonstrating the double ring-cavity Brillouin-FDML laser.

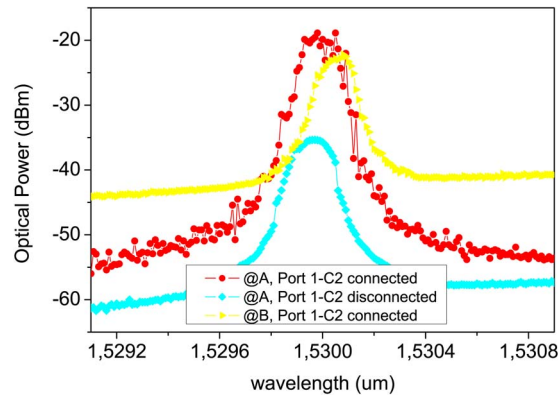


Fig. 4. Measurements of the output optical signal at points A and B (marked in Fig. 3). Data are obtained for the cases when the port 1, of circulator C2, is connected and disconnected. The input power to the FDML ring-cavity was set at 9 dBm.

system. It is observed that the gain of the inset Brillouin fiber ring-laser is affected by the linewidth of the pump source, in this case, the FDML laser.

A center wavelength of 1530 nm was chosen for the experiments by setting  $V_{Bias}$  on the FFP-TF. The first step before generating any Stokes signal was to find the driven frequency for the FDML laser. It was done by disconnecting port 3 of C1 and port 1 of C2; the  $f_d$  of this particular case was measured at 5.025 kHz. Once the FDML laser performance was maximized by setting the correct  $f_d$ , the ring-cavity for the Stokes signal was closed, and the gain of the EDFA was increased for overpassing the Brillouin threshold ( $\sim 9$  dBm). In order to guarantee that the Brillouin scattering was being generated effectively, the process was measured in point A of Fig. 3 when the port 1 of C2 was connected and disconnected; the results of the Brillouin scattering generation are displayed in Fig. 4.

#### 4. Results

The tuning capability of the Brillouin-FDML laser was observed by measuring the output at point A (see Fig. 3) with an input power of 11.8 dBm and  $V_m$  of 12.75 mV. Fig. 5 shows the spectra of the Stokes laser as function of  $V_{Bias}$  applied on the FFP-TF. A tuning range of 200 mV was used to obtain a  $\Delta\lambda_{range}$  of 2.54 nm. In this case, the wavelength range is limited by the gain medium: the EDFA, which does not have a flat gain range all over the C-band. This range could be enlarged for example by using a SOA instead of an EDFA. The Brillouin frequency spectra were measured

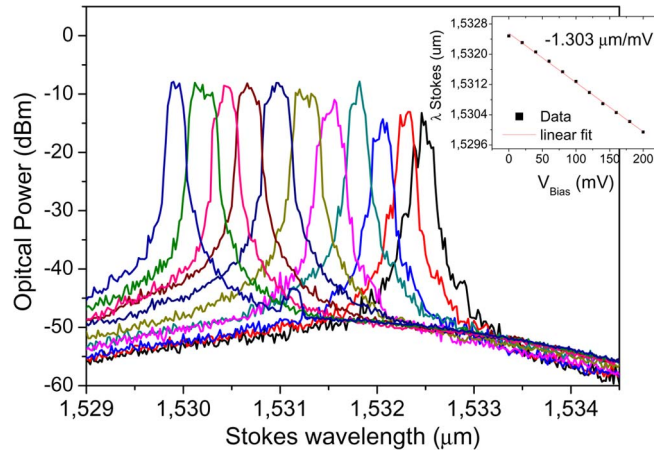


Fig. 5. Output spectra, measured with OSA, of the Stokes laser as function of the bias voltage applied on the FFP-TF.

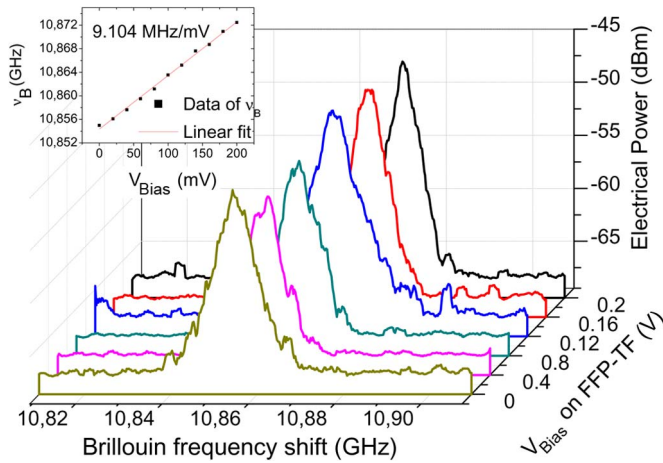


Fig. 6. Brillouin frequency spectra, measured at point A with ESA, measured simultaneously with the Stokes signal of Fig. 5.

simultaneously with the Stokes signal of Fig. 5, and they are presented in Fig. 6. Hence, the tuning variation of the  $\nu_B$  is also demonstrated.

Behavior of laser linewidth using eq. (1) and experimental data are showed in Fig. 7. The linewidth  $\Delta\lambda$  measured for the experimental setup presented in Fig. 3 goes from 0.282 nm to 0.462 nm in a range of 25 mV. Despite that the value for  $V_m = 25$  mV is 30% smaller than the expected value, it is in concordance with a reduction of  $\sim 29.4\%$  in the output power, since the input power, which is the same in all the cases, must be spread in a larger  $\Delta\lambda$ , reducing the output intensity and then the measured linewidth.

Finally, a temporal pulse output of the laser is expected, since the FDML laser output is a frequency swept that can also be seen as a sequence of highly chirped, long pulses with a fixed phase relation between successive frequency sweeps. However, the repetition rate of this Stokes pulses is not necessarily equal to the half driven frequency. It depends on the fiber length  $L$  (the cavity) and the longitude of the backscatter path, the distance that travels the light before being re-injected as the stimulating signal ( $\overline{EDC}$  in Figs. 1 and 3.). If the length  $\overline{EDC}$  is equal to the fiber length, both pulses, the pump and the stimulated, will coincide in the middle point of the fiber  $F$ ;



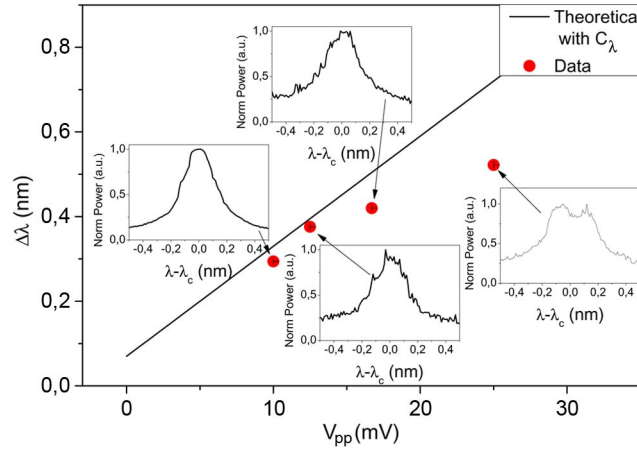


Fig. 7. Linewidth of the Stokes laser at various modulation amplitudes into the FFP-TF.

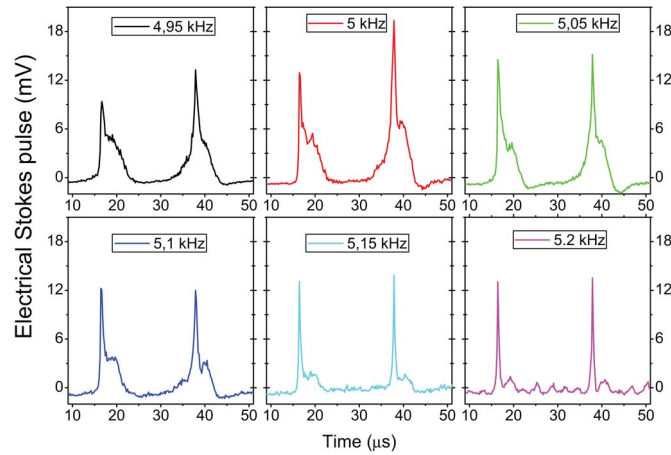


Fig. 8. Temporal profiles of the Stokes laser FDML based.

otherwise, this encounter will be shifted as well as its frequency. The output Stokes pulses were measured replacing the ESA by the oscilloscope, and the data are depicted in Fig. 8. The figure shows the pulse measured for six different driven frequencies, defining the maximum work point of the Stokes pulses and the width of the pulse,  $6.5 \mu\text{s}$  for 5 kHz to  $0.9 \mu\text{s}$  for 5.2 kHz and no pulse for frequencies  $> 5.5 \text{ kHz}$  and  $< 4.9 \text{ kHz}$ . The repetition rate of the Stokes pulses was measured in 4.92 kHz; this value is invariant of the driven frequency.

## 5. Conclusion

In summary, a pulsed and wavelength-tunable Brillouin fiber laser fed by an FDML source was proposed and demonstrated. The tunable laser uses two ring-cavities: One is for the Stokes signal amplification and the other, or the primary fiber-ring cavity, for generating the FDML signal. The pulsed wavelength-tunable Brillouin-FDML fiber laser was implemented using an FFP-TF; an EDFA as the gain medium, working in the C-band; and a standard optical fiber with a length of 18.5 km. These conditions allowed a pulsed Stokes laser, with a repetition rate of 4.2 kHz, center in 1531 nm, with a laser tuning range of 2.54 nm around the central wavelength, by tuning the offset voltage applied to the FFP-F. Additionally, a pulse width of  $6.5 \mu\text{s}$  was measured, with a signal to noise rate

of 10 dB. This pulse is not generated by electrical components. The work here presented offers the possibility of developing a pulsed Brillouin Stokes laser, which can be tuning over a large wavelength range, compact and stable configuration that is coherent with a tuning pump source.

## References

- [1] C. E. Preda, A. A. Fotiadi, and P. Mégret. (2012, Feb.). Numerical approximation for Brillouin fiber ring resonator. *Opt. Exp.* [Online]. 20(5), pp. 5783–5788. Available: <http://www.opticsexpress.org/abstract.cfm?URI=oe-20-5-5783>
- [2] N. A. M. Hambali, M. A. Mahdi, M. H. Al-Mansoori, A. F. Abas, and M. I. Saripan. (2009, Jul.). Investigation on the effect of EDFA location in ring cavity Brillouin-Erbium fiber laser. *Opt. Exp.* [Online]. 17(14), pp. 11 768–11 775. Available: <http://www.opticsexpress.org/abstract.cfm?URI=oe-17-14-11768>
- [3] S. Randoux, V. Lecoecue, B. Ségard, and J. Zemmouri. (1995, Jun.). Dynamical analysis of Brillouin fiber lasers: An experimental approach. *Phys. Rev. A*. [Online]. 51(6), pp. R4345–R4348. Available: <http://link.aps.org/doi/10.1103/PhysRevA.51.R4345>
- [4] Z. Pan, L. Meng, Q. Ye, H. Cai, Z. Fang, and R. Qu. (2009, Mar.). Repetition rate stabilization of the SBS Q-switched fiber laser by external injection. *Opt. Exp.* [Online]. 17(5), pp. 3124–3129. Available: <http://www.opticsexpress.org/abstract.cfm?URI=oe-17-5-3124>
- [5] C. A. Galindez, F. J. Madruga, A. Ullan, M. Lopez-Amo, and J. M. Lopez-Higuera. (2009, Oct.). Temperature sensing in multiple zones based on Brillouin fiber ring laser. *J. Phys., Conf. Ser.* [Online]. 178(1), p. 012017. Available: <http://stacks.iop.org/1742-6596/178/i=1/a=012017>
- [6] F. Zarinetchi, S. P. Smith, and S. Ezekiel. (1991, Feb.). Stimulated Brillouin fiber-optic laser gyroscope. *Opt. Lett.* [Online]. 16(4), pp. 229–231. Available: <http://ol.osa.org/abstract.cfm?URI=ol-16-4-229>
- [7] R. Huber, M. Wojtkowski, and J. G. Fujimoto. (2006, Apr.). Fourier domain mode locking (FDML): A new laser operating regime and applications for optical coherence tomography. *Opt. Exp.* [Online]. 14(8), pp. 3225–3237. Available: <http://www.opticsexpress.org/abstract.cfm?URI=oe-14-8-3225>
- [8] C. Jirauschek, B. Biedermann, and R. Huber. (2009, Dec.). A theoretical description of Fourier domain mode locked lasers. *Opt. Exp.* [Online]. 17(26), pp. 24 013–24 019. Available: <http://www.opticsexpress.org/abstract.cfm?URI=oe-17-26-24013>
- [9] E. J. Lee and Y. P. Kim. (2011, Dec.). Wavelength-tunable and pulse-width variable Fourier domain mode-locking lasers. *Opt. Lett.* [Online]. 36(24), pp. 4752–4754. Available: <http://ol.osa.org/abstract.cfm?URI=ol-36-24-4752>
- [10] E. J. Jung, C.-S. Kim, M. Y. Jeong, M. K. Kim, M. Y. Jeon, W. Jung, and Z. Chen. (2008, Oct.). Characterization of FBG sensor interrogation based on a FDML wavelength swept laser. *Opt. Exp.* [Online]. 16(21), pp. 16 552–16 560. Available: <http://www.opticsexpress.org/abstract.cfm?URI=oe-16-21-16552>
- [11] C. A. Galindez, L. Rodriguez-Cobo, F. Anabitarte, and J. M. Lopez-Higuera, “Integral temperature hybrid laser sensor,” in *Proc. SPIE*, 2012, pp. 842199-1–842199-4. [Online]. Available: <http://dx.doi.org/10.1117/12.975183>
- [12] H. S. Lee, E. J. Jung, S. N. Son, M.-Y. Jeong, and C.-S. Kim, “FDML wavelength-swept fiber laser based on EDF gain medium,” in *Proc. 14th OECC*, 2009, pp. 1–2.
- [13] T. Klein, W. Wieser, B. R. Biedermann, C. M. Eigenwillig, G. Palte, and R. Huber. (2008, Dec.). Raman-pumped Fourier-domain mode-locked laser: Analysis of operation and application for optical coherence tomography. *Opt. Lett.* [Online]. 33(23), pp. 2815–2817. Available: <http://ol.osa.org/abstract.cfm?URI=ol-33-23-2815>
- [14] K. H. Y. Cheng, B. A. Standish, V. X. D. Yang, K. K. Y. Cheung, X. Gu, E. Y. Lam, and K. K. Y. Wong. (2010, Feb.). Wavelength-swept spectral and pulse shaping utilizing hybrid Fourier domain modelocking by fiber optical parametric and erbium-doped fiber amplifiers. *Opt. Exp.* [Online]. 18(3), pp. 1909–1915. Available: <http://www.opticsexpress.org/abstract.cfm?URI=oe-18-3-1909>